JSST
Journal of Space Science and Technology

P-ISSN: 2008-4560
E-ISSN: 2423-4516

Journal of Space Science and Technology

Vol. ??, No. ?, pp. 19-32, 2026
https://doi.org/10.22034/jsst.2025.1581
Journal Homepage: https://jsstpub.com

Original Research Paper

Parametric Resonance of Auxetic Sandwich Cylindrical Structure Subjected to Harmonic Axial Load

Ali Davar and Reza Azarafza[1*]

Faculty of Materials and Manufacturing Technologies, Malek Ashtar University of Technology, Tehran, Iran

ARTICLE INFO

Article History:

Received 13 August 2025
Revised 22 October 2025
Accepted 25 October 2025
Available Online 03 November 2025

Keywords:

Auxetic sandwich structure
Cylindrical shell
Dynamic stability
Mathieu-Hill equations
Harmonic Axial Load

ABSTRACT

In aerospace structures, parametric resonance or dynamic instability, a destructive phenomenon, can occur due to fluctuating excitation sources such as engine thrust. Auxetic materials and structures are increasingly developed in advanced industries such as aerospace and aviation. Due to their negative Poissons's ratio, they show interesting static and dynamic behaviors. In this paper, an auxetic structure is used in the core of a thin sandwich cylindrical shell. The effect of geometric parameters of the unit cell of the cellular auxetic core structure is modeled according to the existing relation for the equivalent mechanical properties. Based on the classical shell theory, the dynamic stability of aluminum three layered sandwich cylindrical shells with auxetic core under combined static and periodic loading is investigated. Expansion of a normal mode for the equations of motion leads to a Mathieu-Hill system of equations. The Bolotin method is employed to determine the instability regions for solving the Mathieu-Hill equations. Validation of the natural frequency and dynamic stability results is performed by comparison with other researchers' publications. Then, parametric study is achieved by studying the influence of the geometric parameters of the unit cell on the dynamic stability of the shell. Results show that the corner angle and dimensional aspect ratio of the unit cell govern the size and origin frequency of the unstable areas.

* Corresponding Author's E-mail: azarmut@mut.ac.ir

How to Cite this Article:
A. Davar and R. Azarafza, "Parametric resonance of auxetic sandwich cylindrical structure subjected to harmonic axial load," *Journal of Space Science and Technology*, Vol. ??, No. ?, pp. 19-32, 2026, https://doi.org/10.22034/jsst.2025.1581.

NOMENCLATURE

SYMBOL	DESCRIPTION
$\boldsymbol{R}$	Cylindrical shell radius
$\boldsymbol{t}$	Cylindrical shell total thickness
$\boldsymbol{L}$	Cylindrical shell length
$\boldsymbol{P_x, P_y, P_z}$	Forces applied to the shell element in axial, circumferential, and radial directions
$\boldsymbol{N_x, N_\theta, N_{x\theta}}$	Resultant normal forces (in axial and circumferential directions) and in-plane shear force
$\boldsymbol{M_x, M_\theta}$ $\boldsymbol{M_{x\theta}}$,	Resultant bending moments in axial and circumferential directions and twisting moment
$\boldsymbol{u, v, w}$	Shell displacement components in axial, circumferential, and radial directions
$\boldsymbol{A_{ij}, B_{ij}, D_{ij}}$	Extensional, coupling and bending stiffness matrix elements
$\boldsymbol{\rho_t}$	Mass density per unit area of the shell
$\boldsymbol{N_a}$	Harmonic axial force
N_0	Constant axial static load
N_s	Oscillatory component of the axial load
N_{cr}	Critical buckling load
P	Excitation frequency (rad/s)
p	Non-dimensional exciting frequency
b_c	Hight of the unit cell (core thickness in radial direction)
h_1, h_2, h_3	Thicknesses of three layered sandwich shell
h_c	Base length of the unit cell
l_c	Leg length of the unit cell
t_c	Unit cell wall thickness
θ_c	Corner angle of the unit cell
E_{11}, E_{22}	Equivalent Young's modulus of the unit cell of the auxetic core in the principal directions (longitudinal and circumferential)
ν_{12}, ν_{21}	Equivalent Poisson's ratios of the unit cell of the auxetic core
G_{12}	Equivalent Shear modulus of the unit cell of the auxetic core

1. INTRODUCTION

Many failures in engineering structures under static or dynamic loading are attributed to structural instability, characterized by large deformations. In studying structural stability, the type of loading dictates the nature of the problem to be solved.

When cylindrical shells are subjected to dynamic loading, they may undergo dynamic buckling and instability. Dynamic buckling occurs if the dynamic load is applied suddenly or changes instantaneously, such as transient loading. The mechanism of dynamic buckling is similar to static buckling, the only difference being the consideration of inertial forces, which results in a lower dynamic buckling load compared to the static buckling load for the same structure. However, if the dynamic load is periodic, i.e., the applied load varies periodically with time, the mechanism, such as dynamic instability, becomes significantly more complex. In static buckling conditions, the critical load is the primary factor causing instability. However, in dynamic conditions, not only the amplitude of the dynamic load vibrations but also the natural vibration frequency and its ratio to the excitation frequency play crucial roles. When the frequency of the dynamic load satisfies the excitation frequency, parametric resonance occurs in the structure, causing the plate or shell to enter a state of dynamic instability.

External loads applied in the equations of motion appear as coefficients and parameters. Consequently, when the loadings are dynamic or time-dependent, the systems are called parametrically excited systems, and instability manifests as parametric instability or parametric resonance.

The growth of internal cracks and the resulting fatigue and failure may ultimately cause dangerous effects on the entire structure. Therefore, for the reliability of structures, investigating the dynamic stability of plates and shells under dynamic loading is of paramount importance. Due to the complexity of the problem, research results in this area are very limited.

Yamaki and Nagai investigated the dynamic stability of a composite cylindrical shell under shear and axial loading in four different boundary conditions using Donnell's equations. They conducted their research using the Galerkin method and solving Hill's equations [1,2]. Ganapati et al. investigated the dynamic stability of curved composite plates. This research examined the influence of fiber angle, number of layers, thickness, and radius of the plates [3]. Kinkayehan investigated the dynamic stability of

a thick cylindrical shell. In this research, the cylindrical shell is also subjected to rotation [4]. In 2022, Hasannezhad and Yazdani Investigated the dynamic compressive (cushioning) response of 3D glass fiber reinforced polymer (GFRP) composites when the shear thickening fluid (STF) matrix base material is modified polyethylene glycol (PEG) [5]. Yazdani and Rahimi, in 2010, experimentally investigated the buckling resistance of reinforced cylindrical shells under axial load. Their investigations concluded that these structures require a minimum density of the lattice for optimal buckling behavior. They also concluded that, under axial loading, the effect of helical stiffeners is greater than that of circumferential stiffeners [6,7]. In 2011, Yazdani and Rahimi experimentally investigated the effect of cyclic axial loading and unloading on simple and stiffened composite shells. Their results indicated that for cyclic loading, stiffened shells exhibited better performance compared to simple shells. Furthermore, the growth of damage was slower in stiffened shells than in simple shells [8]. In 2013, Ghasemi et al. presented a novel method for buckling analysis of stiffened composite shells based on the homogenization method and using first-order shear deformation theory. This method considered the effect of transverse shear forces of the stiffeners. The influence of several geometric parameters on the buckling load was also investigated [9]. In 2015, Rahimi and Taleizadeh proposed a new analytical method for the analysis of stiffened composite shells using the homogenization technique. The main difference between this method and others lies in how the stiffness parameters of the shell and stiffeners are combined to calculate the overall shell stiffness. This method defines a three-layered shell whose volume and stiffness are equivalent to those of the stiffeners. By incorporating these three layers alongside the original shell layers, the overall stiffness can be easily calculated, resulting in less discrepancy with finite element results compared to previous methods [10]. Lam and Ng investigated the dynamic stability of thin, isotropic cylindrical shells under combined static and cyclic axial loading using four common shell theories: Donnell, Love, Sanders, and Flügge. For each theory, the stress distribution due to external loads was considered according to Donnell's theory. The influence of the length-to-radius and thickness-to-radius ratios of the cylinders on instability regions was examined and compared for all four theories [11].

Pellicano studied Dynamic instability of a circular cylindrical shell carrying a top mass under base excitation with Experiments and theory. A theoretical model is developed to reproduce the experimental evidence and provide an explanation of the complex dynamics observed experimentally; the model takes into account geometric shell nonlinearities, electrodynamic shaker equations and the shell shaker interaction [12]. Han et.al. were investigated Dynamic stability of periodic axial loaded cylindrical shell with time-dependent rotating speeds. They were derived utilizing the Donnell's thin shell theory and assumed mode method, the equations of motion for a rotating cylindrical thin shell subjected to time-periodic axial load [13]. Dai and Cao analyzed the parametric stability of rotating cylindrical shells under static and time dependent periodic axial loads. The present work was on the basis of the dynamic version of linear Donnell type equations for thin cylindrical shells under simply-supported boundary conditions. The assumed mode method was employed to reduce the partial differential equations into a system of coupled Mathieu–Hill type equations describing the dynamic instability behaviors of the shell [14]. Mikilyan and Marzocca, were presented dynamic instability of electroconductive cylindrical shells interacting with an external magnetic fields. Two cases of applied external dynamic loads are discussed, namely (i) a harmonic mechanical force, and (ii) a harmonic magnetic field force. Analytical descriptions of the two-dimensional equations and associate conditions of dynamic instability are presented [15]. Heydarpour and Malekzadeh studied the dynamic stability of cylindrical nanoshells subjected to combined static and time-dependent periodic axial forces by employing the two-dimensional nonlocal elasticity theory together with the first-order shear deformation theory of shells. The differential quadrature method, known for its efficiency and accuracy, was applied to discretize the equations of motion under various boundary conditions [16]. Lei et al. analytically investigated the dynamic instability of castellated columns under axial excitation. By assuming instability modes, they formulated the kinetic, strain, and potential

energies of the columns and derived the mass, stiffness, and geometric stiffness matrices of the system [17]. Bakulin and Nedbay proposed a model to study the simultaneous parametric and longitudinal vibrations of an orthotropic cylindrical shell reinforced with longitudinal ribs of piecewise-constant thickness under an axial time-harmonic load. The discrete locations and thickness variations of the ribs have been considered using generalized functions [18]. Zaidan and Hasan presented an analytical study of the parametric instability of cylindrical panels containing functionally graded porous exposed to static and dynamic periodic axial loads under simply supported boundary conditions. Based on Hamilton's principle, the governing equation of motion by using first-order shear deformation theory (FSDT) had been obtained. By applying the Galerkin technique, an excitation frequency expression was derived, which was helped identify areas of instability of functionally graded porous cylindrical panels [19]. Davidson et al. investigated the suppression of parametric resonance in floating bodies utilizing dynamic vibration absorbers, comparing the performance of TMDs against NESs for a test case considering a floating vertical cylinder. In addition to the type of dynamic vibration absorber utilized, the paper also examined the DoF which it acted on, comparing the benefits between attaching the vibration absorber to the primary (heave) DoF or the secondary (pitch) DoF [20]. Sourani et. al. investigated the nonlinear dynamic stability of axially moving carbon nanotube reinforced composite (CNTRC) piezoelectric viscoelastic nano/micro plate under time dependent harmonic biaxial loading. governing equations obtained by using the energy method and Hamilton's principle. An analysis conducted using Galerkin procedure and finally the incremental harmonic balance method to obtain the dynamic instability region [21]. Abdullayev et al. were investigated the loss of stability of multilayer cylindrical shells formed from FG-NC plies on elastic foundation and in thermal environment under lateral pressure based on Donnell type shell theory. The governing partial differential equations derived for cylindrical shells formed from FG-NC plies on two-parameter elastic foundation and assuming the effect of thermal environment were solved by Galerkin procedure and analytical expression was found for critical lateral pressure [22].

While engineers have long explored the dynamic behavior of traditional composite and isotropic cylindrical shells, a gap remains in understanding how sandwich shells with auxetic cores respond, particularly under parametric resonance. Most previous studies have concentrated on buckling under static pressure or crushing during dynamic impact. This research breaks new ground by presenting a three-layer aluminum sandwich cylindrical shell with a re-entrant honeycomb auxetic core, tested under combined steady and vibrating axial loads. This study distinguishes itself by thoroughly examining how the auxetic unit cell geometry, specifically corner angle, wall thickness, and leg length, affects dynamic instability. Using the Mathieu–Hill equation, the research demonstrates that these geometric parameters are not mere structural details but powerful levers for controlling the location, size, and frequency of instability. These findings could be transformative for aerospace components such as rocket interstages and fuselages, where preventing destructive vibrations is essential.

To investigate this, the study develops the equations of motion using classical shell theory and casts them into a system of Mathieu–Hill equations. Bolotin's method is then employed to delineate instability boundaries. A comprehensive parametric study follows, revealing precisely how the auxetic cell geometry influences these critical regions and yielding a practical design guide for engineers developing advanced, vibration-resistant structures.

The paper is organized as follows: Following this introduction, Section 2 details the derivation of the equilibrium equations. Section 3 presents the constitutive equations for the laminated shell and the modeling of the equivalent properties of the auxetic core. The buckling analysis and the formulation for forced vibrations under harmonic load are developed in Sections 4 and 5, respectively, culminating in the Mathieu-Hill system solved via Bolotin's method in Section 6. The validation of the model is presented in Section 7. A detailed discussion of the results from the parametric study is provided in Section 8, and the key conclusions are summarized in Section 9.

2. EQUILIBRIUM EQUATIONS OF THE CYLINDRICAL SHELL

Figure 1 shows a cylindrical shell with mean radius R, total thickness h, and length L, along with its reference coordinates. The mid-surface of the shell is considered the reference surface, and the coordinate system (x, θ, z) is defined on it. u, v, and w are the displacement components in the axial (x), circumferential (θ), and radial (z) directions, respectively, and describe the shell deformation.

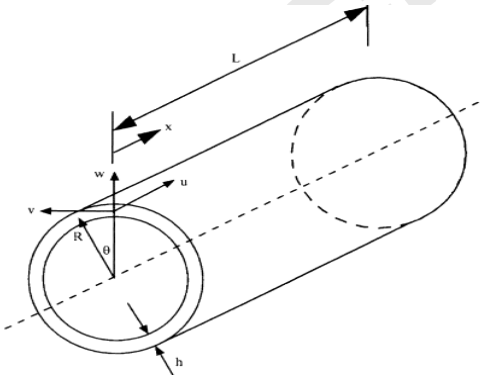

(A)

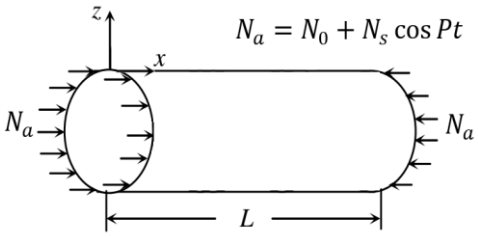

(B)

Fig. 1. (a) Coordinate system of the cylindrical shell [23]; (b) Static and harmonic axial loads.

Figure 2 shows a three-layered sandwich aluminum sandwich cylindrical shell. To obtain the equilibrium equations, it is sufficient to derive the equilibrium equations of forces and moments based on D'Alembert's principle, in the directions of the coordinate axes and about them [24]. The equilibrium equations for cylindrical shells based on bending theory are obtained as [25, 26]:

$$\frac{\partial N_x}{\partial x}+\frac{1}{R}\frac{\partial N_{x\theta}}{\partial \theta}-\rho_t\frac{\partial^2 u}{\partial t^2}=0$$
$$\frac{\partial N_{x\theta}}{\partial x}+\frac{1}{R}\frac{\partial N_\theta}{\partial \theta}+\frac{1}{R}\frac{\partial M_{x\theta}}{\partial x}+\frac{1}{R^2}\frac{\partial M_\theta}{\partial \theta}+N_a\frac{\partial^2 v}{\partial x^2}-\rho_t\frac{\partial^2 v}{\partial t^2}=0 \quad (1)$$
$$\frac{\partial^2 M_x}{\partial x^2}+\frac{2}{R}\frac{\partial^2 M_{x\theta}}{\partial \theta \partial x}+\frac{1}{R^2}\frac{\partial^2 M_\theta}{\partial \theta^2}-\frac{1}{R}N_\theta+N_a\frac{\partial^2 w}{\partial x^2}-\rho_t\frac{\partial^2 w}{\partial t^2}=0$$

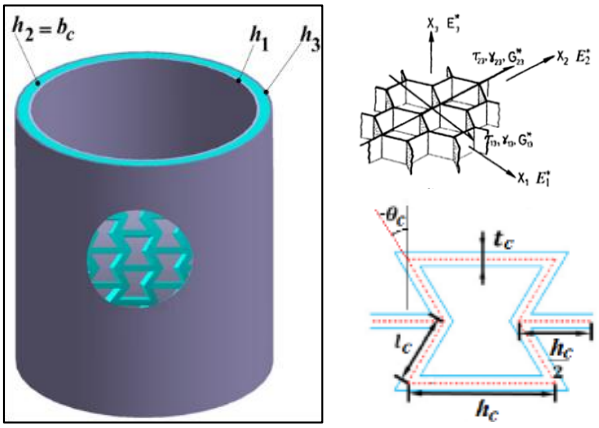

Fig. 2. Three-layered aluminum sandwich cylindrical shell with a core of auxetic cellular structure (Left); Geometric parameters and coordinate system for unit cell of the core structure (Right).

where ρ_t is the mass density per unit area of the shell and $\rho(z)$ the density of the shell:

$$\rho_t = \int_{-h/2}^{h/2} \rho(z)dz \quad (2)$$

$M_x, M_\theta, M_{x\theta}, M_{\theta x}$ are the resultant moments, and N_x, N_θ, $N_{\theta x}$, $N_{x\theta}$, Q_x, Q_θ are the resultant forces. P_z, P_y, P_x are the sums of inertia forces and time-varying external excitations in the z, θ, and x directions, respectively. A constant axial force N_a is assumed to be uniformly distributed over the two end edges of the shell.

3. CONSTITUTIVE EQUATIONS FOR LAMINATED COMPOSITE SHELLS

Figure 3 shows the layer structure of a composite cylindrical shell with thickness h and k layers.

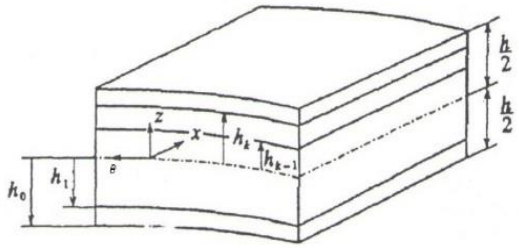

Fig. 3. Layup of a composite cylindrical shell [27].

For a thin-walled shell, the plane stress state is considered, and the corresponding stress-strain relationships are [26, 27]:

$$\{\sigma\} = [\bar{Q}]\{\varepsilon\} \quad (3)$$

where {σ}is the stress vector and {ε} is the strain vector, defined as follows:

$$\{\sigma\}^T = \{\sigma_x, \sigma_\theta, \sigma_{x\theta}\} \quad (4)$$

$$\{\varepsilon\}^T = \{\varepsilon_x\ ,\ \varepsilon_\theta\ , \varepsilon_{x\theta}\} \quad (5)$$

$[\bar{Q}]$ is the reduced transformed stiffness matrix and is defined as: T is the transformation matrix between the principal material coordinates and the shell coordinates and is defined as [27]:

$$T = \begin{bmatrix} \cos^2\theta & \sin^2\theta & 2\sin\theta\cos\theta \\ \sin^2\theta & \cos^2\theta & -2\sin\theta\cos\theta \\ \sin\theta\cos\theta & -\sin\theta\cos\theta & \cos^2\theta - \sin^2\theta \end{bmatrix} \quad (6)$$

In these relationships, θ represents the fiber angle (positive angles are counterclockwise). [Q] is the reduced stiffness matrix and is defined as [28]:

$$[Q_{ij}] = \begin{bmatrix} Q_{11} & Q_{12} & 0 \\ Q_{21} & Q_{22} & 0 \\ 0 & 0 & Q_{66} \end{bmatrix} \quad (7)$$

The Q_{ij} for an orthotropic material are:

$$Q_{11} = \frac{E_{11}}{(1-\nu_{12}\nu_{21})}\ ,\ Q_{22} = \frac{E_{22}}{(1-\nu_{12}\nu_{21})}$$
$$Q_{12} = \frac{\nu_{21}E_{11}}{(1-\nu_{12}\nu_{21})}\ ,\ Q_{66} = G_{12} \quad (8)$$

E_{11} and E_{22} are the elastic moduli in the principal directions, G_{12} is the shear modulus, and ν_{21} and ν_{12} are the Poisson's ratios. The components of the strain vector in Eq.(3) are defined as linear functions of the thickness coordinate z as follows:

$$\varepsilon_x = \varepsilon_1 + zk_1$$
$$\varepsilon_\theta = \varepsilon_2 + zk_2 \quad (9)$$
$$\varepsilon_{x\theta} = \gamma + z\,k_{12}$$

Where $\varepsilon_x, \varepsilon_\theta, \varepsilon_{x\theta}$ are the axial, hoop, and in-plane shear strains, respectively. $\varepsilon_1, \varepsilon_2, \gamma$ are the mid-surface strains, and k_1, k_2, k_{12} are the mid-surface curvatures. The strain relationships are [29]:

$$\varepsilon_x = \frac{\partial u}{\partial x} - z\frac{\partial^2 w}{\partial x^2}$$
$$\varepsilon_\theta = \frac{1}{R}\left(\frac{\partial v}{\partial \theta} + w\right) - z\frac{1}{R^2}\frac{\partial^2 w}{\partial \theta^2} \quad (10)$$
$$\varepsilon_{x\theta} = \frac{\partial v}{\partial x} + \frac{1}{R}\frac{\partial u}{\partial \theta} - z\frac{2}{R}\frac{\partial^2 w}{\partial x \partial \theta}$$

The relationships between the resultant forces and moments are defined based on classical lamination theory as [28]:

$$\begin{Bmatrix} N_x \\ N_\theta \\ N_{x\theta} \\ M_x \\ M_\theta \\ M_{x\theta} \end{Bmatrix} = \begin{bmatrix} A_{11} & A_{12} & A_{16} & B_{11} & B_{12} & B_{16} \\ A_{21} & A_{22} & A_{26} & B_{21} & B_{22} & B_{26} \\ A_{16} & A_{26} & A_{66} & B_{16} & B_{26} & B_{66} \\ B_{11} & B_{12} & B_{16} & D_{11} & D_{12} & D_{16} \\ B_{21} & B_{22} & B_{26} & D_{21} & D_{22} & D_{26} \\ B_{16} & B_{26} & B_{66} & D_{16} & D_{26} & D_{66} \end{bmatrix} \begin{Bmatrix} \varepsilon_1 \\ \varepsilon_2 \\ \gamma \\ k_1 \\ k_2 \\ \tau \end{Bmatrix} \quad (11)$$

$$(A_{ij}, B_{ij}, D_{ij}) = \int_{-h/2}^{h/2} Q_{ij}(1, z, z^2)dz \quad (i,j = 1,2,6) \quad (12)$$

Using the strain-displacement relations (10) in equation (11), we obtain the following relations [29]:

$$N_x = A_{11}\frac{\partial u}{\partial x} + \frac{A_{12}}{R}\left(\frac{\partial v}{\partial \theta} + w\right) - B_{11}\frac{\partial^2 w}{\partial x^2} - \frac{B_{12}}{R^2}\frac{\partial^2 w}{\partial \theta^2}$$
$$N_\theta = A_{12}\frac{\partial u}{\partial x} + \frac{A_{22}}{R}\left(\frac{\partial v}{\partial \theta} + w\right) - B_{12}\frac{\partial^2 w}{\partial x^2} - \frac{B_{22}}{R^2}\frac{\partial^2 w}{\partial \theta^2}$$
$$N_{x\theta} = \frac{A_{66}}{R}\frac{\partial u}{\partial \theta} + A_{66}\frac{\partial v}{\partial x} - \frac{2B_{66}}{R}\frac{\partial^2 w}{\partial x \partial \theta}$$
$$M_x = B_{11}\frac{\partial u}{\partial x} + \frac{B_{12}}{R}\left(\frac{\partial v}{\partial \theta} + w\right) - D_{11}\frac{\partial^2 w}{\partial x^2} - \frac{D_{12}}{R^2}\frac{\partial^2 w}{\partial \theta^2} \quad (13)$$
$$M_\theta = B_{12}\frac{\partial u}{\partial x} + \frac{B_{22}}{R}\left(\frac{\partial v}{\partial \theta} + w\right) - D_{12}\frac{\partial^2 w}{\partial x^2} - \frac{D_{22}}{R^2}\frac{\partial^2 w}{\partial \theta^2}$$
$$M_{x\theta} = \frac{B_{66}}{R}\frac{\partial u}{\partial \theta} + B_{66}\frac{\partial v}{\partial x} - \frac{2D_{66}}{R}\frac{\partial^2 w}{\partial x \partial \theta}$$

Substituting relations (13) into equations (1), the equilibrium equations are summarized as follows [29]:

$$\begin{bmatrix} L_{11} & L_{12} & L_{13} \\ L_{21} & L_{22} & L_{23} \\ L_{31} & L_{32} & L_{33} \end{bmatrix} \begin{Bmatrix} u \\ v \\ w \end{Bmatrix} = \begin{Bmatrix} -Rp_x \\ -Rp_y \\ -Rp_z \end{Bmatrix} \quad (14)$$

L_{ij} are differential operators.

4. BUCKLING ANALYSIS OF COMPOSITE CYLINDRICAL SHELL

To perform the buckling eigenvalue analysis, the time-dependent terms must first be eliminated from the equilibrium equations. The initial membrane stress resultants σ_x^i are assumed to be defined as follows [30]:

$$N_x^i = \sigma_x^i h \tag{15}$$

We assume the existence of a load parameter N_0^i (or the unknown eigenvalue) such that:

$$\sigma_x^i = k_x \frac{N_0^i}{h} \tag{16}$$

And consequently:

$$N_x^i = \sigma_x^i h = k_x N_0^i \tag{17}$$

k_x is a constant describing the load and it is equal to -1. To perform the buckling analysis, the initial external forces from eq. (17) are substituted into the equilibrium eq. (1). Then, similar to the free vibration analysis, for each value of m and n, a system of equations is obtained as follows [30]:

$$\begin{aligned}
&\int_0^L \int_{-\pi}^{\pi} \left(L_{11}u + L_{12}v + L_{13}w - k_x N_0^i\right) U dx d\theta = 0 \\
&\int_0^L \int_{-\pi}^{\pi} \left(L_{21}u + L_{22}v + L_{23}w - k_\theta N_0^i\right) V dx d\theta = 0 \\
&\int_0^L \int_{-\pi}^{\pi} \left(L_{31}u + L_{32}v + L_{33}w - k_z N_0^i\right) W dx d\theta = 0
\end{aligned} \tag{18}$$

By integration and coefficient grouping, the following eigenvalue equation is obtained [30]:

$$[[G]_{mn} - N_0^i [E]_{mn}]\{\Delta\}_{mn} = [\gamma']_{mn}\{\Delta\}_{mn} = 0 \tag{19}$$

By setting the determinant of the matrix $[\gamma']_{mn}$ equal to zero, the frequency equation for the cylindrical shell with the desired boundary conditions is obtained:

$$det\,[\gamma']_{mn} = 0 \Rightarrow C_1 {N_0^i}^3 + C_2 {N_0^i}^2 + C_3 N_0^i + C_4 = 0 \tag{20}$$

Solving this equation yields the critical buckling load of the composite cylindrical shell; the minimum value is considered the acceptable critical buckling load.

5. FORCED VIBRATIONS OF A of a COMPOSITE CYLINDRICAL SHELL UNDER HARMONIC AXIAL FORCE

The alternating (harmonic) axial force per unit length is given by:

$$N_a = N_0 + N_s \cos Pt \tag{21}$$

where P is the excitation frequency in radians per second. The equations of motion can be solved using the eigen function expansion of the normal modes of a cylindrical shell under a constant axial load N_0 with an oscillatory component $N_s = 0$. To solve the equations of motion including the oscillatory component N_s, a solution of the following form is considered, which incorporates the response for all mode shapes [30]:

$$\begin{aligned}
u_{mnj} &= \sum_{j=1}^{3}\sum_{m=1}^{\infty}\sum_{n=1}^{\infty} A_{mnj} q_{mnj}(t) \cos\lambda_m x \cos n\theta \\
v_{mnj} &= \sum_{j=1}^{3}\sum_{m=1}^{\infty}\sum_{n=1}^{\infty} B_{mnj} q_{mnj}(t) \sin\lambda_m x \sin n\theta \\
w_{mnj} &= \sum_{j=1}^{3}\sum_{m=1}^{\infty}\sum_{n=1}^{\infty} C_{mnj} q_{mnj}(t) \sin\lambda_m x \cos n\theta
\end{aligned} \tag{22}$$

where $q_{mnj}(t)$ are the generalized coordinates. Substituting the above three equations into Eqs. (14) yields [28]:

$$\sum_{j=1}^{3}\sum_{m=1}^{\infty}\sum_{n=1}^{\infty}\left(\ddot{q}_{mnj} + \omega_{mnj}^2 q_{mnj}\right)\alpha_{mnj}\cos\lambda_m x \cos n\theta = 0 \tag{23}$$

$$\sum_{j=1}^{3}\sum_{m=1}^{\infty}\sum_{n=1}^{\infty}\left(\ddot{q}_{mnj} + \omega_{mnj}^2 q_{mnj}\right)\beta_{mnj}\sin\lambda_m x \sin n\theta = 0$$

$$\sum_{j=1}^{3}\sum_{m=1}^{\infty}\sum_{n=1}^{\infty}\left(\ddot{q}_{mnj} + \omega_{mnj}^2 q_{mnj}\right)\sin\lambda_m x \cos n\theta - \frac{1}{\rho_t}\lambda_m \cos Pt \sum_{j=1}^{3}\sum_{m=1}^{\infty}\sum_{n=1}^{\infty} q_{mnj}\frac{\partial}{\partial x}(N_s \cos\lambda_m x)\cos n\theta = 0$$

We define:

$$\alpha_{mnj} = \frac{A_{mnj}}{C_{mnj}} \quad , \quad \beta_{mnj} = \frac{B_{mnj}}{C_{mnj}} \tag{24}$$

Using the orthogonality condition, we multiply the first row of Eq. (23) by $\alpha_{rsi}\cos\lambda_r x\cos s\theta$, the second row by $\beta_{rsi}\sin\lambda_r x\sin s\theta$, and the third row by $\sin\lambda_r x\cos s\theta$. The resulting equations are equivalent to [31]:

$$M_{IJ}\ddot{q}_J + \left(K_{IJ} - cosPtQ_{IJ}\right)q_J = 0 \quad (25)$$

where M_{IJ} ،K_{IJ} ،Q_{IJ} are matrices, and $\ddot{q}_J$ and q_J are column vectors. This system of equations is known as the Mathieu-Hill equation. The subscripts *r, s, i, m, n, j, I, J* have the following values (ranges):

$$\begin{aligned} r,s,m,n &= 1,2,3,4,\dots,N \\ i,j &= 1 \\ I,J &= 1,2,3,4,\dots,(N\times N\times 3) \end{aligned} \quad (26)$$

The matrices M_{IJ} ،k_{IJ} ،Q_{IJ} are given by [31]:

$$\begin{aligned} &M_{IJ} \\ &= \int_0^l \int_0^{2\pi} \left(\alpha_I\alpha_J\, cos\,\lambda_r x\, cos\, s\theta\, cos\,\lambda_m x\, cos\, n\theta\right. \\ &+ \beta_I\beta_J\, sin\,\lambda_r x\, sin\, s\theta\, sin\,\lambda_m x\, sin\, n\theta \\ &\left.+ sin\,\lambda_r x\, cos\, s\theta\, sin\,\lambda_m x\, cos\, n\theta\right) d\theta dx \\ &= \begin{cases} \pi L/2\left(1+\beta_I\beta_J+\alpha_I\alpha_J\right) & I=J \\ 0 & I\neq J \end{cases} \end{aligned} \quad (27)$$

$$\begin{aligned} &K_{IJ} = \omega_J^2 M_{IJ} \\ &Q_{IJ} = \frac{1}{\rho_t}\lambda_m \int_0^L \int_0^{2\pi} \frac{\partial}{\partial x}\left(N_s\, cos\,\lambda_m x\, cos\, n\theta\right) \\ &\quad sin\,\lambda_r x\, cos\, s\theta\, d\theta dx \\ &\quad = \begin{cases} -\pi L/(2\rho_t)\lambda_r\lambda_m N_s & I=J \\ 0 & I\neq J \end{cases} \end{aligned} \quad (28)$$

6. SOLVING THE FORCED HARMONIC MATHIEU-HILL VIBRATION EQUATIONS

The response with period $2T$ is of greater practical importance due to the width of these instability regions, which are usually larger than the regions of responses with period T. Using the first-order Bolotin approximation, periodic responses with period 2T can be written as:

$$f = a\,sin\frac{PT}{2} + b\,cos\frac{PT}{2} \quad (29)$$

where a and b are arbitrary vectors. Substituting eq. 29 into equation 25 and equating the coefficients of $\cos\frac{PT}{2}$ and $\sin\frac{PT}{2}$ yields a set of homogeneous linear algebraic equations in a and b. The condition for non-trivial solutions is: where zero is an $N\times N$ null matrix [31]. To obtain nontrivial solutions for P, the following conditions should be satisfied:

$$\begin{vmatrix} K_{IJ} - \frac{1}{2}Q_{IJ} - \frac{1}{4}P^2M_{IJ} & 0 \\ 0 & K_{IJ} + \frac{1}{2}Q_{IJ} - \frac{1}{4}P^2M_{IJ} \end{vmatrix} = 0 \quad (30)$$

Non-dimensional exciting frequency is defined as:

$$p = 2\pi RP\left(\frac{\rho_t}{A_{11}}\right)^{1/2} \quad (31)$$

Where A_{11} is extentional stiffness of the shell. The material properties relations of the auxetic cellular structure of the core of the sandwich cylindrical shell shown in Fig. 1, used in the present study, could be found in Ref. [32]. Based on the above analytical formulation, a MATLAB code is written and analytical results are obtained.

7. VERIFICATION

To verify the dynamic stability of the structure, the fundamental instability frequency and the span angle of this region are calculated using Eq. (30) by the Mathieu-Hill method and compared with the results of the reference article as indicated in Tab. 1. In this case, a constant initial force N_0 is applied to the structure along the length of the cylindrical shell, the value of which is $\pm 0.1\,N_{cr}$ and $\pm 03\,N_{cr}$. The modulus of elasticity and the characteristics of the cylindrical shell are as follows [33]:

$E_1/E_2 = 40$, $G_{12}/E_2 = 0.5$, $\upsilon_{12} = 0.25$

$\rho = 3450\ kg/m^3$, $R/h = 200$, $L/R = 2$,

Layup: [90/0]

Critical buckling load is considered as follows:

$$N_{cr} = \frac{E_2 h^2}{R[3(1-\upsilon_{12}{}^2\upsilon_{21}{}^2)]^{1/2}}$$

Table 1. Comparison of dynamic instability regions of a composite laminated cylindrical shell using the present theory and ref. [33].

Static axial force	Present				Lam and Ng [33]			
	(m,n)=(1,6)		(m,n)=(1,5)		(m,n)=(1,6)		(m,n)=(1,5)	
	Bifurcation frequency parameter	Opening Angle (rad) $*10^{-2}$	Bifurcation frequency parameter	Opening Angle (rad) $*10^{-2}$	Bifurcation frequency parameter	Opening Angle (rad) $*10^{-2}$	Bifurcation frequency parameter	Opening Angle (rad) $*10^{-2}$
$N_0 = 0.1\ N_{cr}$	5.81074	2.40793	6.07059	2.27786	5.65441	2.40955	5.95966	2.29713
$N_0 = 0.3\ N_{cr}$	5.90197	7.11215	6.15905	6.73543	5.75054	7.12689	6.05093	6.77495
$N_0 = -0.1\ N_{cr}$	5.71952	2.44634	5.98490	2.31047	5.55663	2.46345	5.86696	2.33335
$N_0 = -0.3\ N_{cr}$	5.62553	7.46165	5.89367	7.03872	5.45709	7.50755	5.77278	7.09944

The maximum discrepancy in Tab. 1 is less than 3% since Ref. [33] used Love theory of cylindrical shells.

8. RESULT AND DISCUSSION

Unless otherwise stated, the geometry and material specifications applied in the present study are

- R=3m, L=3m, $h_1 = h_3$=0.5mm.
- Auxetic parameters: b_c=h_2=60mm, hc=60mm, l_c=30mm, t_c=3mm, $\theta_c = -45^{\circ}$.
- Equivalent orthotropic properties of the auxetic core are E_{11}=72.65GPa, E_{22}=225.5GPa, G_{12}=6.25GPa, υ_{12}=-0.54,υ_{21}= -1.67, ρ=590.7kg/m^3.

Material properties of aluminum: E=69GPa, $\upsilon = 0.33$ and $\rho = 2700\ kg/m^3$

The effect of axial compressive force on the dynamic instability regions of the shell for a unit cell corner angle (θ) of -45 degrees is investigated in Fig. 4. This figure shows the ratio of the dynamic force amplitude to the critical buckling force (vertical axis) as a function of the dimensionless excitation frequency parameter (horizontal axis). As shown in this figure, with an increase in the axial compressive force, the bifurcation frequency decreases, the instability region shifts to the left, and the area of the instability region increases. In the proceeding figures, the instability parameters are investigated versus the dimensionless ratio of the static axial compressive force (N_0/N_{cr}).

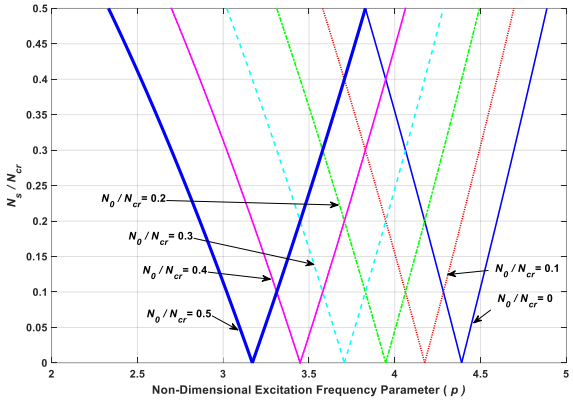

Fig. 4. Effect of axial compressive force on the dynamic instability regions of the shell.

Figure 5 illustrates the area of the instability region as a function of the dimensionless ratio of the static axial compressive force.

As observed in Fig. 5, with a change in the auxetic unit cell corner angle from -60 degrees to +60 degrees, the maximum area of the instability region corresponds to an angle of +60 degrees, and the minimum area corresponds to an angle of -45 degrees. Furthermore, with an increase in the dimensionless ratio of the axial compressive force, the size of the instability region increases for all corner angles.

Figure 6 depicts the effect of the corner angle on the bifurcation frequency curve as a function of the dimensionless ratio of the axial compressive force. As observed, in this figure, in contrast to Fig. 5, the

dependence of the increase in bifurcation frequency on the corner angles is reversed as compared to the dependence of the size of the unstable region area. Also, unlike Fig. 5, in this figure, with an increase in the dimensionless ratio of the axial compressive force, the bifurcation frequency decreases.

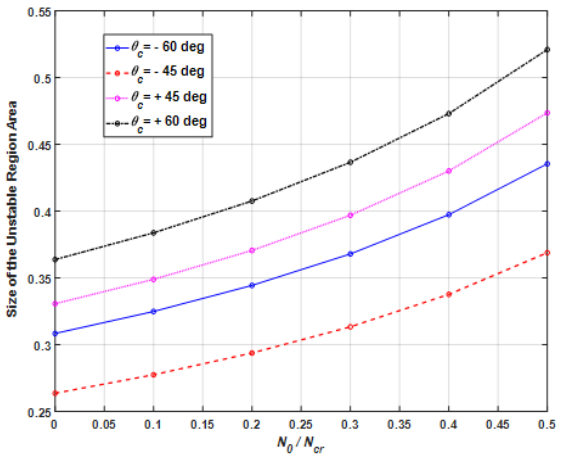

Fig. 5. Effect of the corner angle of the unit cell on the area of the instability region.

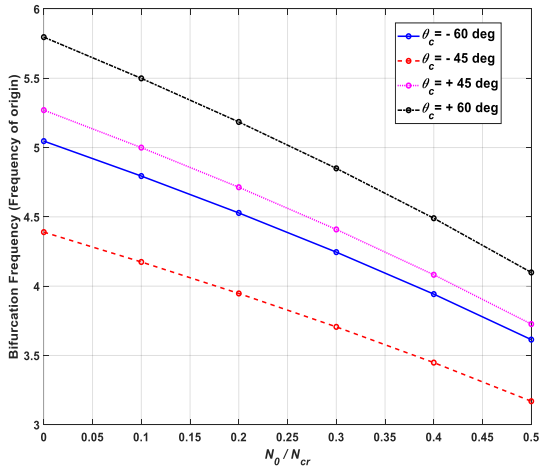

Fig. 6. Effect of the corner angle of the unit cell on the bifurcation frequency curve.

Figures 7 and 8 show the effect of the unit cell wall thickness on the area of the instability region and the bifurcation frequency, respectively, as a function of the dimensionless axial compressive force. As can be seen in these figures, unlike the dependence shown in Figs. 5 and 6 on the unit cell corner angle parameter, the dependence of the area of the instability region and the bifurcation frequency on the increase in unit cell wall thickness is similar. Also, similar to Figs. 5 and 6, in Figs 7 and 8, the area of the instability region and the bifurcation frequency increase and decrease, respectively, with increasing dimensionless axial compressive force.

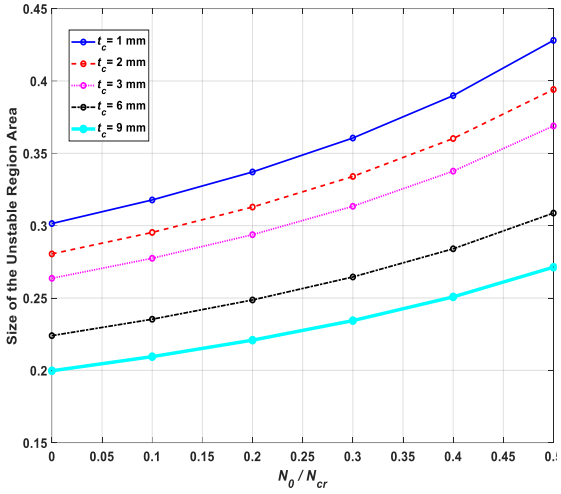

Fig. 7. Effect of the unit cell wall thickness on the area of the instability region.

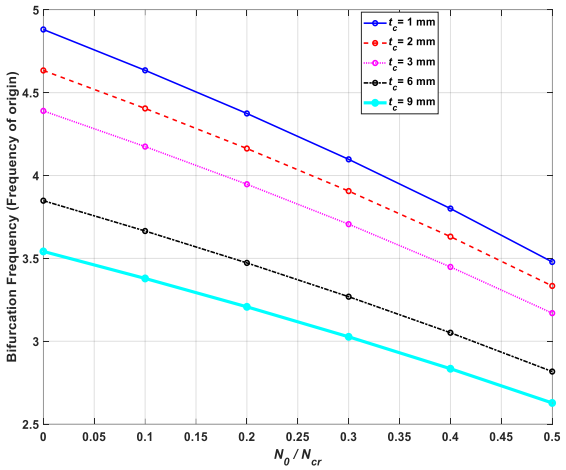

Fig. 8. Effect of the unit cell wall thickness on bifurcation frequency curve.

Figure 9 shows the curve of the area of the instability region for different mode numbers. As can be seen, with an increase in the number of longitudinal half-waves m, for all circumferential mode numbers n, the area of the instability region increases. Also, for longitudinal half-waves m=1 to m=5, with an increase in the circumferential wave number n, the area of the

instability region first increases and then decreases. However, for longitudinal half-waves m greater than 5, with an increase in the circumferential wave number n, the area of the instability region decreases.

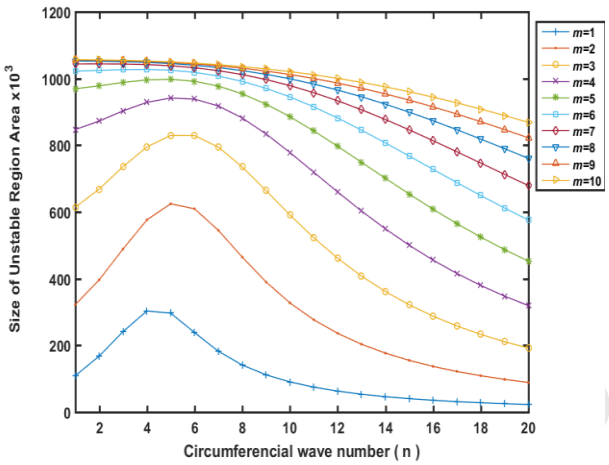

Fig. 9. Variations of the size of the area of the instability region for different mode numbers (m,n); ($\frac{N_0}{N_{cr}} = 0.25$).

As indicated in Fig. 10, by increasing the value of n, at smaller values of m, the bifurcation frequency is first decreased and then increased. But for larger values of m, the bifurcation frequency is monotonically increased.

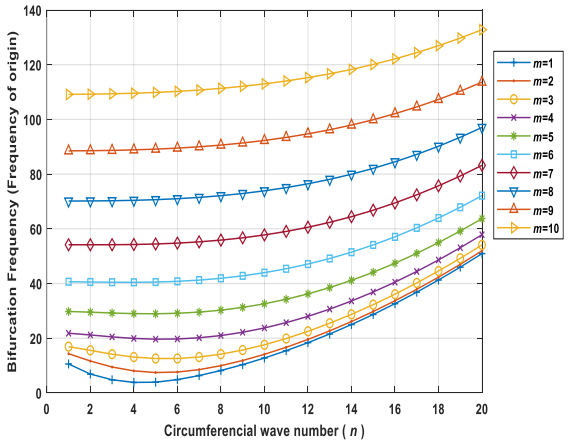

Fig. 10. Variations of the bifurcation frequency of the instability region for different mode numbers (m,n); ($\frac{N_0}{N_{cr}} = 0.25$).

As shown in Fig. 11, regardless of the value of n, by increasing the values of m, the value of the opening angle at bifurcation point of the unstable region is increased. At higher values of m, the opening angle is less sensitive with respect to n. But at lower values of m, the variation of the opening angle is more and it is first increased and the decreased as the value of n is increased.

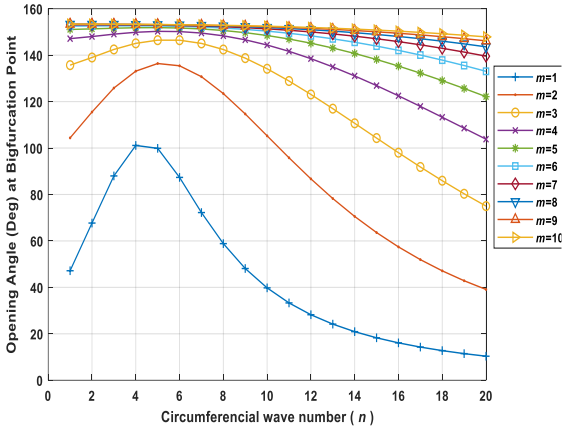

Fig. 11. Variations of the opening angle (Deg) at bifurcation point for different mode numbers (m,n).

Three-dimensional plot of the unstable region surrounded between upper and lower boundary surfaces is depicted in Fig. 12. According to this figure, by increasing the value of the static axial compressive load (N_0), the bifurcation frequency at the intersection of the upper and lower surfaces is decreased, while the size of the unstable region is increased.

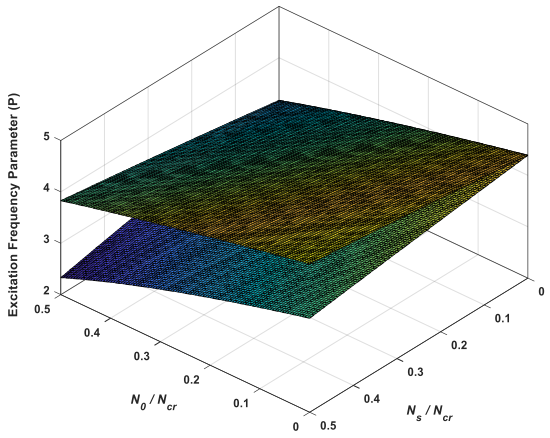

Fig. 12. Three-dimensional plot of the unstable region surrounded between upper and lower boundary surfaces.

As indicated in Fig. 13, for all the values of the unit cell leg length (l_c), by increasing the value of the static axial compressive load (N_0),

the value of the opening angle at bifurcation point of the unstable region is increased. This increment is slightly nonlinear and it is more at higher values of l_c.

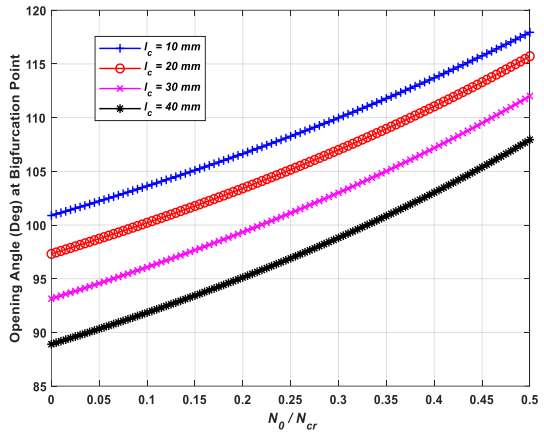

Fig. 13. Effect of the unit cell leg length (l_c) on the opening angle at bifurcations point of the instability region.

Effect of the unit cell leg length (lc) on the dimensionless buckling load parameter ($N_{cr}/E_{22}h$) for the critical axial buckling mode number (m=2) is illustrated in Fig. 14. According to this figure, by increasing l_c, for all the values of n, the buckling load parameter is increased. Also, irrespective to the value of l_c, by increasing the value of n, the buckling load parameter is first decreased and the increased.

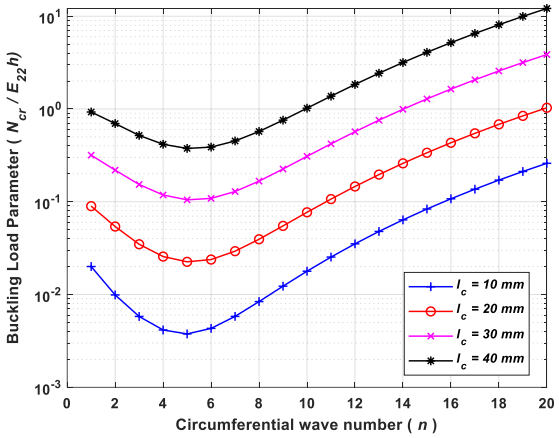

Fig. 14. Effect of the unit cell leg length (l_c) on the dimensionless buckling load parameter ($N_{cr}/(E_{22}h)$), (m=2).

Figure 15 shows the effect of the unit cell leg length (l_c) on the dimensionless natural frequency parameter for the bending vibration mode number (m=1). As it can be seen in this figure, in contrast to Fig. 14, by increasing l_c, for all the values of n, the natural frequency parameter is decreased. Also, irrespective to the value of l_c, by increasing the value of n, the natural frequency parameter is first decreased and the increased. At l_c=40mm, eventually the mode number corresponded to the fundamental frequency is changed.

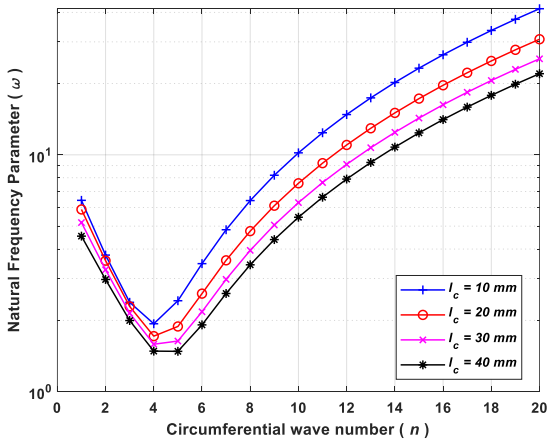

Fig. 15. Effect of the unit cell leg length (l_c) on the dimensionless natural frequency parameter (m=1, $\frac{N_0}{N_{cr}} = 0.25$).

9. CONCLUSION

This paper investigates the dynamic instability of three-layered sandwich cylindrical shells made of aluminum with an auxetic core, subjected to a combined static and harmonic axial load, based on classical shell theory. The influence of unit cell geometric parameters, including corner angle and wall thickness, on the instability region area and bifurcation frequency was studied. The results showed that for all values of the unit cell geometric parameters, increasing the static compressive axial load increases the instability region area and decreases the bifurcation frequency. Furthermore, it can be inferred that positive and negative corner angles can significantly affect the dynamic instability behavior of the shell. The unit cell leg length is a crucial parameter influencing the dynamic instability behavior of auxetic cylindrical shells. The results show that variations in the unit cell leg length cause opposite effects on the buckling load and natural frequency of auxetic cylindrical shells. In summary, the main innovations of this

study are as follows:

- Novel Material Application: To the best of our knowledge, this is the first investigation into the parametric resonance behavior of sandwich cylindrical shells featuring an auxetic core. While auxetic materials have been explored extensively for their static mechanical properties, their response to dynamic instability under harmonic axial loading remains largely unexplored—making this work a step into new territory.
- Tailorable Dynamic Stability: Our results reveal that the regions of dynamic instability- a critical concern for aerospace structures- are not fixed. Instead, they can be purposefully tuned by adjusting the geometric parameters of the auxetic core. In particular, the corner angle (θ_c), wall thickness (t_c), and leg length (l_c) of the unit cell emerge as key design levers for controlling stability.
- Engineering Insight: From a design standpoint, the findings offer practical guidance: employing a core with a negative Poisson's ratio (for example, θ_c = -45°) results in a smaller instability region and a higher bifurcation frequency compared to a positive Poisson's ratio. This translates to improved robustness against parametric resonance—an advantage especially relevant to aerospace components such as rocket interstages and aircraft fuselages exposed to varying thrust or aerodynamic forces.

CONFLICTS OF INTEREST

The authors declare that they have no conflict of interest.

REFERENCES

[1] N. Yamaki and K. Nagai, "Dynamic stability of circular cylindrical shells under periodic shearing forces," *Journal of Sound and Vibration*, vol. 45, no. 4, pp. 513-527, 1976, https://doi.org/10.1016/0022-460X(76)90732-X.

[2] K. Nagai and N. Yamaki, "Dynamic stability of circular cylindrical shells under periodic compressive forces," *Journal of Sound and Vibration*, vol. 58, no. 3, pp. 425-441, 1978, https://doi.org/10.1016/S0022-460X(78)80048-0.

[3] M. Ganapathi, T. K. Varadan, and V. Balamurugan, "Dynamic instability of laminated composite curved panels using finite element method," *Computers & Structures*, vol. 53, no. 2, pp. 335-342, 1994, https://doi.org/10.1016/0045-7949(94)90206-2.

[4] Q. Han, Z. Qin, J. Zhao, and F. Chu, "Parametric instability of cylindrical thin shell with periodic rotating speeds," *International Journal of Non-Linear Mechanics*, vol. 57, pp. 201–207, 2013, https://doi.org/10.1016/j.ijnonlinmec.2013.08.002.

[5] H. Hasannezhad and M. Yazdani, "Investigate the dynamic compressive (cushioning) response of 3D GFRP composites when the STF matrix base material is modified PEG," *Journal of Molecular Liquids*, vol. 366, 2022, Art. no. 120304, https://doi.org/10.1016/j.molliq.2022.120304.

[6] M. Yazdani, H. Rahimi, A. A. Khatibi, and S. Hamzeh, "An experimental investigation into the buckling of GFRP stiffened shells under axial loading," *Scientific Research and Essays*, vol. 4, no. 9, pp. 914-920, 2009.

[7] M. Yazdani and G. H. Rahimi, "The effects of helical ribs number and grid types on the buckling of thin-walled GFRP-stiffened shells under axial loading," *Journal of Reinforced Plastics and Composites*, vol. 29, no. 17, pp. 2568-2575, 2010, https://doi.org/10.1177/0731684409355202.

[8] M. Yazdani and G. H. Rahimi, "The behavior of GFRP-stiffened and-unstiffened shells under cyclic axial loading and unloading," *Journal of Reinforced Plastics and Composites*, vol. 30, no. 5, pp. 440-445, 2011, https://doi.org/10.1177/0731684411398537.

[9] M. A. Ghasemi, M. Yazdani, and M. Hoseini, "Analysis of effective parameters on the buckling of grid stiffened composite shells based on first order shear deformation theory," *Journal of Modares Mechanical Engineering*, vol. 13, no. 10, pp. 51-61, 2014, (in Persian).

[10] A. Talezadehlari and Gh. H. Rahimi, "Buckling analysis of stiffened composite cylindrical shell based on the modifieds smear method," *Journal of Modares Mechanical Engineering*, vol. 15, no. 11, pp. 319-329, 2016, (in Persian).

[11] K. Y. Lam and T. Y. Ng, "Dynamic stability of cylindrical shells subjected to conservative periodic axial loads using different shell tsheories," *Journal of Sound and Vibration*, vol. 207, no. 4, pp. 497-520, 1997, https://doi.org/10.1006/jsvi.1997.1186.

[12] F. Pellicano, "Dynamic instability of a circular cylindrical shell carrying a top mass under base excitation: Experiments and theory," *International Journal of Solids and Structures*, vol. 48, no. 3–4, pp. 408-427, 2011, https://doi.org/10.1016/j.ijsolstr.2010.09.024.

[13] Q. Han, Z. Qin, W. Lu, and F. Chu, "Dynamic stability analysis of periodic axial loaded cylindrical shell with time-dependent rotating speeds,"

Nonlinear Dynamics, vol. 81, no. 4, pp. 1649–1664, 2015, https://doi.org/10.1007/s11071-015-2097-y.

[14] Q. Dai and Cao, "Parametric instability of rotating cylindrical shells subjected to periodic axial loads," *International Journal of Mechanical Sciences*, vol. 146–147, pp. 1-8, 2018, https://doi.org/10.1016/j.ijmecsci.2018.07.031.

[15] M. Mikilyan and P. Marzocca, "Dynamic instability of electroconductive cylindrical shell in a magnetic field," *International Journal of Solids and Structures*, vol. 160, no. 15, pp. 168-176, 2019, https://doi.org/10.1016/j.ijsolstr.2018.10.022.

[16] Y. Heydarpour and P. Malekzadeh, "Dynamic stability of cylindrical nanoshells under combined static and periodic axial loads," *Journal of the Brazilian Society of Mechanical Sciences and Engineering*, vol. 41, no. 4, 2019, Art. no. 184, https://doi.org/10.1007/s40430-019-1675-1.

[17] J. S. Lei, B. Kim, and L. y. Li, "Dynamic instability analysis of axially compressed castellated columns," *International Journal of Steel Structures*, vol. 20, no. 2, pp. 559–566, 2020, https://doi.org/10.1007/s13296-020-00306-8.

[18] V. N. Bakulin and A.Y. Nedbay, "Dynamic stability of a cylindrical shell reinforced by longitudinal ribs of piecewise-constant thickness under axial loading," *Doklady Physics*, vol. 65, no. 12, pp. 436–441, 2020, https://doi.org/10.1134/S1028335820120034.

[19] S. M. Zaidan and H. M. Hasan, "Parametric instability of functionally graded porous cylindrical panels under the effect of static and time-dependent axial loads," *Vibration*, vol. 5, no. 3, pp. 570-584, 2022, https://doi.org/10.3390/vibration5030033.

[20] J. Davidson, T. Kalmár-Nagy, and G. Habib, "Parametric excitation suppression in a floating cylinder via dynamic vibration absorbers: a comparative analysis," *Nonlinear Dynamics*, vol. 110, no. 2, pp. 1081–1108, 2022, https://doi.org/10.1007/s11071-022-07710-1.

[21] P. Sourani, A. Ghorbanpour Arani, M. Hashemian, and S. Niknejad, "Nonlinear dynamic stability analysis of axially moving CNTRC piezoelectric viscoelastic Nano/Micro plate based on MCST," *Journal of Computational Applied Mechanics*, vol. 55, no. 2, pp. 242-274, 2024, https://doi.org/10.22059/jcamech.2023.367406.896.

[22] G. I. Abdullayev, M. Avey, Y. I. Aliyev, I. R. Mamedov, and A. H. Sofiyev, "Loss of stability of multilayer cylindrical shells formed from nanocomposite layers in various environments under lateral pressure," *Journal of Applied and Computational Mechanics*, 2025, https://doi.org/10.22055/jacm.2025.48472.5257.

[23] K. Y. Lam and C. T. Loy, "Influence of boundry conditions for a thin laminated rotating cylindrical shell," *Composite Structure*, vol. 41, no. 3-4, pp. 215-228, 1998, https://doi.org/10.1016/S0263-8223(98)00012-9.

[24] S. Timoshenko and S. Woinowsky-Krieger, *Theory of Plates and Shells*, 2rd ed. USA, McGraw-Hill, 1989.

[25] M. Farshad, *Design and Analysis of Shell Structures*, 1rd ed. Netherlands: Springer, 1992, https://doi.org/10.1007/978-94-017-1227-9.

[26] A. C. Ugural, *Stresses in Plate and Shells*, 2nd ed. Boston: WCB/McGraw-Hill, 1999.

[27] J. R. Vinson, *The Behavior of Shells Composed of Isotropic and Composite Materials*, 1st ed. Springer, 1993, https://doi.org/10.1007/978-94-015-8141-7.

[28] S. M. Mohseni Shakib, *Analysis and Design of Composite Structures*, 4rd ed. Tehran, Iran: Imam Hossein University Press, 2017, (in Persian).

[29] R. Ruotolo, "A comparison of some thin shell theories used for the dynamic analysis of stiffened cylinders," *Journal of Sound and Vibration*, vol. 243, no. 5, pp. 847-860, 2001, https://doi.org/10.1006/jsvi.2000.3447.

[30] A. W. Leissa, *Vibration of Shells*, NASA SP-288, National Aeronautics and Space Administration, 1973.

[31] L. Meirovitch, *Fundamentals of Vibration*, McGraw-Hill, 2001.

[32] L. J. Gibson and M. F. Ashby, *Cellular Solid Structure and Properties,* Cambridge University Press, 1999, pp. 162-166.

[33] K. Y. Lam and T. Y. Ng, "Dynamic stability analysis of laminated composite cylindrical shells subjected to conservative periodic axial loads," *Composites Part B: Engineering*, vol. 29, no. 6, pp. 769-785, 1998, https://doi.org/10.1016/S1359-8368(98)00033-XGet rights and content.